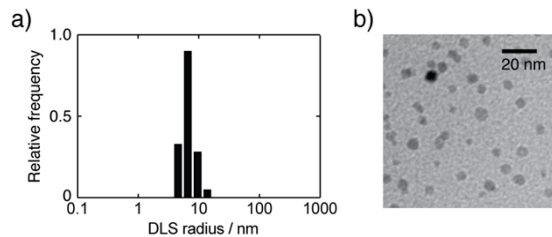


## SUPPORTING INFORMATION

<b>Table of Contents</b>	<b>page</b>
Figure S1: Size characterization of pcLCIO nanoparticles	2
Figure S2: Functional instability of sensors based on uncrosslinked lipid coated iron oxide nanoparticles	3
Figure S3: Sequence of DsRed-RS20.v3	4
Figure S4: Aggregation rate measured for a sensor containing 50 $\mu\text{M}$ Fe, 12.5 $\mu\text{M}$ DsRed-RS20.v3, and 3.75 $\mu\text{M}$ CaM at 37 °C	5
Figure S5: Calcium sensitivity titration curve	6
Supplemental Methods	7
Supplemental References	13

**Figure S1.** Size characterization of pcLCIO nanoparticles. (a) Dynamic light scattering (DLS) mass-weighted size histogram showing a mean pcLCIO particle radius of  $8.3 \pm 1.5$  nm. (b) Transmission electron microscopy image of pcLCIOs with intrinsic contrast showing 5-10 nm electron dense cores. Scale bar = 20 nm.



**Figure S2.** Functional instability of sensors based on uncrosslinked lipid coated iron oxide nanoparticles. (a) Sensors formed with  $\sim 16$  nm CaM-LCIO and RS20-LCIO nanoparticles aggregated to approximately 200 nm mean cluster size after addition of 500  $\mu\text{M}$   $\text{CaCl}_2$  (final concentration), but then appeared to fall apart spontaneously after roughly 15 minutes incubation; no precipitate was visible. (b) 500  $\mu\text{M}$   $\text{Ca}^{2+}$  was added to CaM-LCIO/RS20-LCIO mixtures preincubated initially in 100  $\mu\text{M}$  EDTA (black), 1  $\mu\text{M}$  EDTA (gray), or 100  $\mu\text{M}$  EGTA (magenta) for the indicated amounts of time. For preincubation periods  $\geq 10$  min, little calcium-dependent aggregation could subsequently be observed, suggesting the possibility of exchange or displacement of proteins conjugated to the particle surfaces.

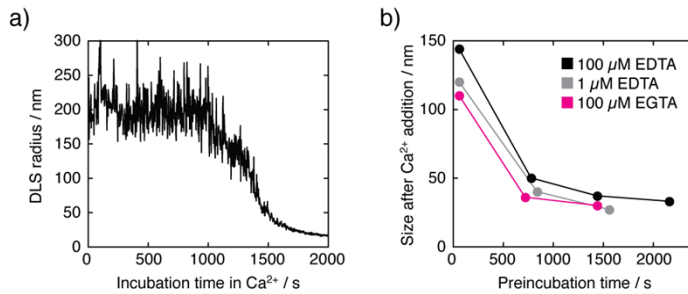


**Figure S3.** Sequence of DsRed-RS20.v3. Regions corresponding to the hexahistidine tag, DsRed, and RS20 are color coded in blue, magenta, and green, respectively. Locations of the two charge reversal mutations included in this variant and the intermediate DsRed-RS20.v2 variant are highlighted with shaded boxes: K249E (v2 and v3) and K188E (v3 only).

```
1 MGSSHHHHHH SSSLVDPGSH MASSEDIKE FMRFKVRMEG SVNGHEFEIE
51 GEGEGRPYEG TQTAKLKVTK GGPLPFAWDI LSPQFQYGSK VYVKHPADIP
101 DYKKLSFPEG FKWERVMNFE DGGVVTVTQD SSLQDGSFIY KVKFIGVNF
151 SDGPVMQKKT MGWEASTERL YPRDGLKGE IHKALKLEDG GHYLVEFKSI
201 YMAKKPVQLP GYYYVDSKLD ITSHNEDYTI VEQYERAEGR HHLFLGSSEG
251 GRRKWQKTGH AVRAIGRLSS S
```

**Figure S4.** Aggregation rate measured for a sensor containing 50  $\mu\text{M}$  Fe, 12.5  $\mu\text{M}$  DsRed-RS20.v3, and 3.75  $\mu\text{M}$  CaM at 37  $^{\circ}\text{C}$ . A monoexponential curve was fit to the average of two independent DLS traces (red line, s.e.m. indicated by shading). The fit (black line) indicated an effective rate of  $0.252 \pm 0.004 \text{ min}^{-1}$ .

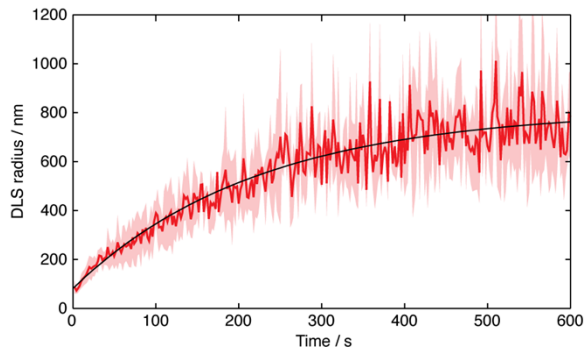
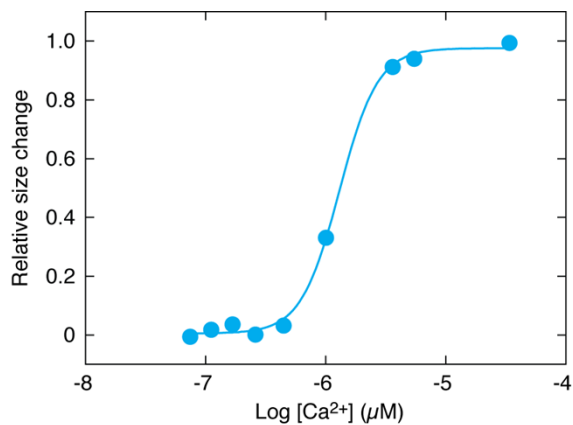


**Figure S5.** Calcium sensitivity titration curve measured by DLS to determine the  $EC_{50}$  of the calcium sensors. DLS was performed at 37 °C after 5 min of mixing the sensors containing 150  $\mu\text{M}$  Fe, 5  $\mu\text{M}$  DsRed-RS20.v3, and 0.75  $\mu\text{M}$  CaM. Solutions with different  $\text{Ca}^{2+}$  concentrations were formulated using commercial calibration buffers. The calculated  $EC_{50}$  for  $\text{Ca}^{2+}$  was 1.3  $\mu\text{M}$ , as determined by fitting the data to a non-depleting two state model of calcium binding by the sensors.



## SUPPLEMENTAL METHODS

**Supplies.** Magnetic iron oxide ( $\text{Fe}_3\text{O}_4$ ) nanoparticles with a reported diameter of 5 nm were purchased from Sigma-Aldrich (St. Louis, MO). 1,2-distearoyl-*sn*-glycero-3-phosphoethanolamine-N-[maleimide(polyethylene glycol)-2000] (DSPE-PEG-maleimide) and 1,2-bis(10,12-tricosadiynoyl)-*sn*-glycero-2-phosphoethanolamine-N-[maleimide(polyethylene glycol)-2000] (23:2 diyne PE-PEG-maleimide) were obtained in lyophilized form from Avanti Polar Lipids (Huntsville, AL), the latter following custom synthesis. Additional chemicals were purchased from Sigma-Aldrich unless otherwise noted.

**Lipid coated iron oxide nanoparticle preparation.** Uncrosslinked lipid coated iron oxide (LCIO) nanoparticles and photocrosslinked lipid coated iron oxide (pcLCIO) particles were prepared using similar procedures. Solutions of DSPE-PEG-maleimide (LCIOs) or 23:2 diyne DSPE-PEG-maleimide (pcLCIOs) were prepared in  $\text{CHCl}_3$  (8 mg/mL) and then added to a suspension of 5 nm diameter iron oxide particles initially in toluene. Mixtures were brought to a 1:20 ratio of  $\text{Fe}_3\text{O}_4$  to lipids (w:w), with a final iron concentration of 0.4 mg/mL. For procedures involving 23:2 diyne DSPE-PEG-maleimide, sample containers were wrapped in aluminum foil in order to protect them from light exposure. Lipid-iron oxide mixtures were dried overnight in a hood. Dried films were resuspended to a concentration of approximately 1.5 mM Fe in 10 mM 4-(2-hydroxyethyl)-1-piperazineethanesulfonic acid (HEPES), pH 7.2 buffer, with 150 mM NaCl. Solutions were filtered through a  $\mu$ MACS magnetic column (Miltenyi Biotec,

Auburn, CA) to remove aggregated species and the flow-through fractions were filtered using 0.2  $\mu\text{m}$  mesh Whatman Anotop syringe filters (GE Healthcare, Piscataway, NJ). Maleimide groups on the surface of the particles were quantified using ultrasensitive thiol and sulfide quantification kit from Life Technologies (Grand Island, NY). Photocrosslinking or control mock-crosslinking procedures were performed by flushing the samples with argon for 15 min and transferring them to a 1 mm quartz cell, followed by irradiation for 40 minutes at 254 nm using an 8 W ultraviolet (UV) lamp placed 10 cm from the cuvette. UV-visible spectroscopy was used to follow the time-course of the photocrosslinking reaction. In order to eliminate empty phospholipid micelles and vesicles, samples were ultracentrifugated for 20 min at 173,000g; supernatants were discarded and the particles were resuspended in HEPES buffer.

Nanoparticle iron oxide concentrations were determined using a colorimetric assay based on the iron chelator bathophenanthrolinedisulfonic acid (BPS).<sup>1</sup> Nanoparticle stability was assessed by dynamic light scattering (DLS)-based functional assays and by challenging crosslinked or mock-crosslinked particles at a concentration of 0.5 mM Fe with 50% ethanol for one hour, followed by 5 minutes centrifugation at 3,000g. Transmission electron micrographs of pLCIO samples on carbon grids were obtained using standard methods on a JEOL (Tokyo, Japan) 2010 Advanced High Performance transmission electron microscope.

**Protein preparation and conjugation.** N-terminally hexahistidine tagged and cysteine modified calmodulin (CaM) from *Xenopus laevis* was recombinantly expressed in *E. coli* and purified using Ni-affinity chromatography as described previously.<sup>2</sup> Purity was

assessed by sodium dodecyl sulfate polyacrylamide gel electrophoresis (SDS-PAGE) following a standard protocol, and protein concentration was measured using the Pierce 660 nm Assay (Thermo Fisher Scientific, Rockford, IL). Purified CaM at concentrations of 21, 42, 85, 170, or 340  $\mu$ M was added LCIOs or pcLCIOs at 25 mg/mL Fe and incubated for 2 hours at room temperature. Cystamine (11 mg/mL) was added to the particles and incubated for 30 min to quench any free maleimide groups remaining after the CaM conjugation. To remove unconjugated protein, the resulting samples were dialyzed against 1 L of 1 mM HEPES, pH 7.2, 150 mM NaCl for 12 hours, including one buffer change. Finally, samples were filtered using 0.2  $\mu$ m syringe filters. Final protein concentration conjugated to the nanoparticles was measured using the Pierce 600 nm Assay, and iron concentration was estimated using the BPS assay.

DsRed-RS20 fusion proteins (Supplemental Fig. S3) were constructed by fusing residues the CaM-binding domain of chicken smooth muscle myosin light chain kinase, known as the RS20 peptide (RRKWQKTGHAVRAIGRLSSS), to the C-terminus of an N-terminally polyhistidine tagged fusion of DsRed-Express,<sup>2</sup> an enhanced variant of the red fluorescent protein DsRed. Vectors were based on the commercial expression plasmid pET28a (Novagen, Madison, WI). Site directed mutagenesis within the coding sequence for DsRed-RS20 was performed by polymerase chain reaction and blunt ligation. *E. coli* BL21(DE3)Star cells (Life Technologies) carrying the resulting plasmid were inoculated from an overnight culture at a 1:100 ratio into Luria-Bertani medium supplemented with 100  $\mu$ g/mL kanamycin, and were grown with vigorous shaking for approximately 3 hours at 37 °C until they reached an OD<sub>600</sub> ~0.6. Cultures were induced with 1 mM isopropyl  $\beta$ -D-1-thiogalactopyranoside with vigorous shaking for 3 hours at 30 °C followed by gentle

shaking incubation overnight at 4 °C to maximize chromophore maturation. Inclusion bodies were prepared from harvested cell pellets by lysing in BugBuster (Novagen) with lysozyme and benzonase, following the manufacturer's protocol, followed by centrifugation of the resultant crude lysate at 16000 x *g* for 20 minutes. The pelleted inclusion bodies were then solubilized in Pierce Inclusion Body Solubilization Reagent (Thermo Scientific) and batch affinity purified by incubating the solubilized protein with Ni-NTA agarose resin (Qiagen, Valencia CA) under denaturing conditions for 1-2 hours. The resin was then washed in two column volumes of Solubilization Reagent, refolded on column by washing the resin-bound protein in 50 mM sodium phosphate, 300 mM NaCl, 20 mM imidazole, pH 8. Refolded protein was then eluted in an otherwise identical buffer containing 250 mM imidazole. Protein purity was assessed by SDS-PAGE, and protein concentration was determined using the Pierce 660 nm Protein Assay. Isoelectric points (pI values) were estimated using the Scripps Protein Calculator available online.

**Light-Scattering Experiments.** Dynamic light scattering (DLS) measurements were performed using a DynaPro DLS system (Wyatt Technology, Santa Barbara, CA). Reported particle diameters were obtained from mass-weighted histograms (Fig. 2e and Supplemental Fig. S1) or by extracting single intensity-weighted size parameters from the DLS data (all other figures). Intensity-weighted values were greater than mass-weighted sizes, but could be obtained from fewer time points and were thus most suitable for kinetic measurements. Mixtures of DsRed-RS20 and CaM-LCIO or CaM-pcLCIO variants were formed in 10 mM HEPES, pH 7.2, supplemented with 200 mM NaCl and 250  $\mu$ M EDTA, except where noted otherwise. Further doses of EDTA or CaCl<sub>2</sub> were

added as noted in the text and figure captions. Mixing dead time for DLS kinetic experiments was approximately 3 s. All DLS measurements were performed at 37 °C.

**MRI experiments.** Samples containing CaM-pcLCIO and DsRed-RS20 variants were formulated as described above, with concentrations of components including EDTA and CaCl<sub>2</sub> as noted in the text and figure captions. Aliquots were arrayed into microtiter plates; unused wells were filled with buffer to avoid susceptibility artifacts in imaging. Plates were then placed into a 9 cm inner diameter birdcage coil in a 40-cm-bore Bruker (Billerica, MA) Avance 4.7 T MRI scanner equipped with 12 cm inner diameter triple axis 26 G/cm gradients, and imaging was performed on a 2 mm slice positioned through halfway through the sample height. A  $T_2$ -weighted spin echo pulse sequence with multiecho acquisition was used; repetition time ( $TR$ ) was 2 s, and echo time ( $TE$ ) ranged from 10 to 300 ms. Data matrices of 256 x 128 points were acquired with an in-plane resolution of 200 x 400  $\mu\text{m}$ . MRI image time series were obtained after mixing and setup dead time of 4 min, and with an acquisition time of 4 min per scan. MRI experiments were performed at 22 °C.

**Aggregation model calculations.** The aggregation kinetics of binary nanoparticle sensors were simulated in two scenarios, using a Brownian dynamics approach<sup>1</sup> implemented in Matlab. In the symmetric binary scenario, 24 particles of radius 8 nm, classified as either type A or type B particles (12 of each), were simulated such that each particle type could bind to exclusively to the opposite type. In the asymmetric binary scenario, 24 type A particles were paired with 96 crosslinking domains of a smaller 4 nm

radius (type C), again such that each species could bind exclusively to the opposite type. The ratio of particles to crosslinking domains in the asymmetric scenario was chosen such that the interaction surface area on the two species was equal. Simulations began with particles sited in a uniform random distribution within a 300 nm cubic box with periodic boundary conditions. Positions were adjusted over 20,000 time steps of 5 ns each. At each step, each particle was moved in a random direction by a distance equal to its mean 5 ns diffusion path length, given the diffusion constant calculated by the Stokes-Einstein relation and assuming a viscosity of  $1.02 \times 10^{-3}$  Pa-s and temperature of 293 K. A discontinuous bonding probability function was chosen, such that approach of complementary particles to within 1% of the sum of their diameters resulted in a “bond” being formed. Correct bond distances and the absence of overlap among particles were ensured at each diffusion step by also applying an elastic spring force to resolve violations,<sup>1</sup> assuming a constant mass density of  $1.4 \text{ g/cm}^3$  for each particle.

**Data analysis.** MRI scans were reconstructed and analyzed in Matlab (Mathworks, Natick, MA).  $T_2$  relaxation rates ( $R_2$ ) were determined by exponential fitting to signal amplitudes as a function of echo time, and relaxivity values were determined by linear fitting to a graph of  $R_2$  vs. concentration for nanoparticles imaged at 0-320  $\mu\text{M}$  Fe. Further data analysis and figure generation were performed with Matlab, Kaleidagraph (Synergy Software, Reading, PA), and Adobe Creative Suite (Adobe Systems, San Jose, CA).

## SUPPLEMENTAL REFERENCES

- [1] Tamarit, J.; Irazusta, V.; Moreno-Cermeno, A.; Ros, J. *Anal Biochem* **2006**, *351*, 149-51.
- [2] Pflieger, B.F.; Fawzi, N.J.; Keasling, J.D. *Biotechnol Bioeng* **2005**, *92*, 553-8.